

LOW-PROFILE DIRECTIONAL ULTRA-WIDEBAND ANTENNA FOR SEE-THROUGH-WALL IMAGING APPLICATIONS

F. Zhu^{1,*}, S. Gao¹, A. T. S. Ho², T. W. C. Brown³, J. Z. Li⁴, and J. D. Xu⁴

¹Surrey Space Centre, University of Surrey, Guildford, GU2 7XH, UK

²Department of Computing, University of Surrey, Guildford, GU2 7XH, UK

³Centre for Communication Systems Research, University of Surrey, GU2 7XH, UK

⁴Northwestern Polytechnical University, Xi'an 710072, China

Abstract—A compact-size planar antenna with ultra-wideband (UWB) bandwidth and directional patterns is presented. The antenna can be fabricated on a printed circuit board (PCB). On one side of the PCB, it has a circular patch, and on the other side it has a slot-embedded ground plane with a fork-shaped feeding stub in the slot. Directional radiation is achieved by using a reflector below the antenna. To reduce the thickness of the antenna, a new low-profile antenna configuration is proposed. Three types of directional UWB antennas are analyzed. The distance between the antenna and the reflector is 12 mm ($0.16\lambda_0$, λ_0 is the free space wavelength at the lowest frequency). In order to validate the design, a prototype is also fabricated and measured. Measured results agree well with the simulated ones. The measured results confirm that the proposed antenna features a reflection coefficient below -10 dB over the UWB range from 4.2 GHz to 8.5 GHz, a maximum gain around 9 dBi, a front-to-back ratio over 17 dB and pulse fidelity higher than 90% in the time domain. Thus it is promising for see-through-wall imaging applications.

Received 9 August 2011, Accepted 13 October 2011, Scheduled 19 October 2011

* Corresponding author: Fuguo Zhu (zhu.fuguo@hotmail.com).

1. INTRODUCTION

Ultra-wideband through the wall imaging (TWI) radar has attracted much attention in both academic and industrial communities as it has important applications in homeland security, fire and rescue in collapsed buildings and natural disaster situations such as earthquakes and hurricanes [1].

There are a few companies and laboratories which work on the UWB TWI radars. Involved systems and prototypes include the following: 1) Radar Vision 1000 [2] and 2000 [3] from Time Domain Company; 2) Prism 200 [4] from Cambridge Cons.; 3) ImpSAR [5] from Eureka Aerospace Company; 4) Xaver 800 [6] from Camero Technology. Among them, Xaver 800 is the latest product which operates from 3 GHz to 10 GHz. It provides high resolution images of 20 mm through most common wall materials. Novelda Company [7] produces some UWB radar modules which can be integrated with UWB antennas.

In addition to those listed above, the following laboratories/universities are also working on the UWB TWI radars: Defence R&D Canada, Kyoto University, Delft University of Technology, University of Tennessee, and Center for Advanced Communications at Villanova University. A real-time see-through-wall radar system [8] based on FPGA is designed and implemented in the University of Tennessee. It covers dual frequency bands. One frequency range extends from 2 GHz to 4 GHz; the other frequency range is from 7 GHz to 13 GHz.

The UWB frequency band from 3.1 to 10.6 GHz with the maximum power spectral density of -41.3 dBm/MHz allocated by the Federal Communications Commission (FCC) has accelerated the research of UWB radar system since 2002 [9]. In the UK, the Office for Communications (OfCom) also established a standard in 2007 for UWB radars [10]. The UK OfCom regulations defines a frequency range for UWB radar which includes a 600 MHz band centered at 4.5 GHz, and a 2.5 GHz band centered at 7.25 GHz. Compared with traditional radar, UWB radar has many advantages such as high resolution, resistance to multipath phenomenon, extremely low power emission and low power consumption.

The design of directional UWB antennas is the key issue of UWB radars. Though many UWB antennas are available in the literature, most of them are for UWB communications which require omnidirectional patterns. The aim of this project is to investigate novel designs of low-cost and small antennas suitable for UWB through the wall imaging radars.

Main challenges of the UWB antenna design for radars include impedance matching, low distortion of pulses, directional patterns,

high front-to-back ratio for rejecting false alarms from the movement of the user holding the device, compact size and low cost. In the literature, the widely used antennas for UWB radar are horn [11, 12] and Vivaldi antennas [8, 13, 14]. Both types of antennas can produce broadband impedance matching and directional patterns. The horn antenna is bulky in size, while the Vivaldi antenna is planar and can be easily implemented in arrays. In [13, 14], a 16×16 antipodal Vivaldi antenna array antenna has been used at the receiver for UWB through wall imaging with synthetic aperture radar (SAR) algorithm. However, Vivaldi antenna is large in size as it has to be at least a few wavelengths at the lowest frequency for obtaining directional radiations and good impedance matching [14]. Other directional wideband antennas include coaxial fed suspended patch antennas [15–18], and cavity backed antennas [19–21]. Some techniques to achieve directional patterns are available in the literature, which include the use of lossy absorbing materials [22] or a reflector below the radiating element [23–26]. The use of lossy absorbing material, however, may lead to low radiation efficiency. Regarding the use of reflectors, different types of reflectors have been used, such as corner reflector [23], pyramidal reflecting ground plane [24] and planar reflector [25, 26]. Compared with the use of corner reflector and pyramidal reflector ground plane, the directional UWB antenna with a planar reflector has low fabrication cost and is easy to implement in UWB arrays. In [26], a directional UWB array has been realized by using four pairs of leaf-shaped bowtie elements and a flat aluminium plate as a reflector. Recently, various planar monopoles have been reported [27–31]. In [32], a compact UWB UHF array antenna has been developed for through wall radar by using the printed elliptical monopole antenna. However, it performs a bidirectional pattern without a shielding element. Reported in [33], a small size directional antenna has been proposed for UWB wireless personal area networks (WPAN) and wireless body area networks (WBAN) by employing a slot monopole antenna and a small size reflector. It has a poor front-to-back ratio (< 10 dB) due to its small size reflector.

The main problem of the directional UWB antenna with a reflector is the thickness of the antenna, as the reflector usually needs to be located at a distance of about $1/4$ wavelength from the antenna [23]. For portable radar system applications, it is necessary to reduce both the thickness and the size of the antenna, which is the motivation of this work.

In this paper, a low profile directional UWB antenna is proposed. The paper is organized as follows: Section 2 shows the configurations and comparisons of two reference antennas with directional patterns.

A novel directional UWB antenna is proposed in Section 3. The results of parametric study and analysis of current distribution are carried out in this section. Both simulated and measured results of reflection coefficients and radiation patterns are illustrated in Section 4. The transient result of the proposed directional UWB antenna demonstrates its capability for impulse radar system. Section 5 gives the conclusion.

2. CONFIGURATION AND RESULTS OF TWO REFERENCE ANTENNAS

This section will discuss two reference antennas added with reflectors, and the performance will be compared with the proposed antenna in Section 3. In [34], the bandwidth enhancement of slot antenna can be categorized into two types. One is to manipulate the field distribution in the slot with a circular patch (as Reference Antenna 1 shown in Fig. 1). The other is to use a circular slot and a fork-like stub for excitation (as Reference Antenna 2 shown in Section 2.2). The radiation patterns of both antennas are omni-directional in H -plane and bi-directional in E -plane. The directional patterns can be achieved by adding a reflector. In this section, two kinds of reference antennas with reflector are investigated respectively.

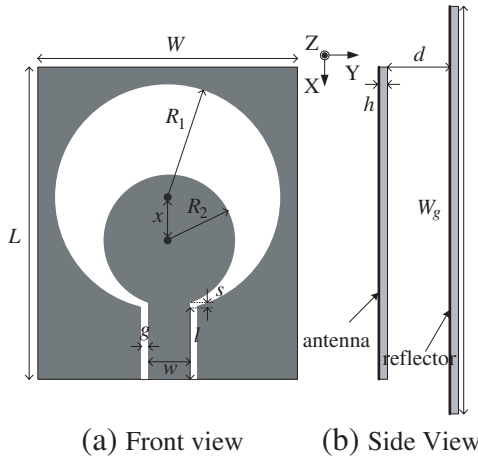


Figure 1. Configuration of reference UWB antenna with reflector. (Reference Antenna 1).

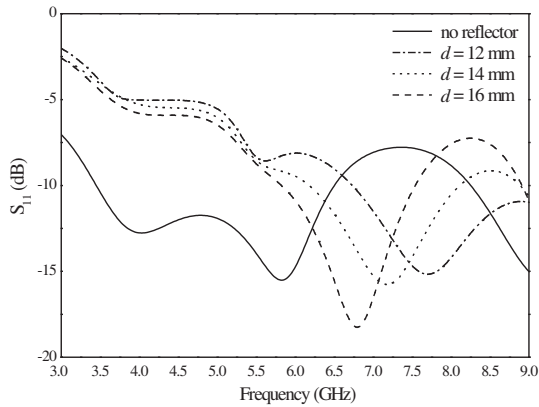


Figure 2. Simulated reflection coefficients in terms of d compared to the case of no reflector. (Reference Antenna 1).

2.1. Reference Antenna 1 — Coplanar Waveguide (CPW) Fed UWB Slot Antenna

Figure 1 shows the configuration of reference UWB antenna with a reflector. This antenna is denoted as reference antenna 1. The optimal value of s should not be larger than the thickness of the substrate h [31]. The Duroid5880 substrate with dielectric constant of 2.2 and thickness of 1.575 mm is used in this project. The frequency band of the designed UWB antenna is from 4.2 GHz to 8.5 GHz which covers the UWB band of OfCom, UK. The slot aperture depends on the lowest frequency of operation ($f_1 = 4.2$ GHz) approximately [31]:

$$R_1 \approx \frac{c}{4f_1 \sqrt{\frac{1+\epsilon_r}{2}}} \times \frac{2}{\pi} \tag{1}$$

$$R_2 \approx \frac{R_1}{2} \tag{2}$$

Dimensions of the UWB antenna are as follows: $W = 30$ mm, $L = 34$ mm, $R_1 = 13.7$ mm, $R_2 = 7.5$ mm, $x = 5.3$ mm, $w = 3.6$ mm, $g = 0.2$ mm, $l = 5.45$ mm, $s = 1.0$ mm. To achieve directional patterns, the reflector with a dimension of 50 mm \times 50 mm is added to increase the directivity. Fig. 2 shows the effect of various distances between reflector and antenna on the reflection coefficients versus frequency. It shows that, compared to the original antenna without a reflector, the impedance matching of the antenna has been strongly affected by the reflector, especially at lowest frequencies. The lowest frequency for $S_{11} < -10$ dB shifts from 6.7 GHz to 5.8 GHz when the distance

increases from 12 mm to 16 mm, however, this leads to a bulky antenna.

2.2. Reference Antenna 2 — UWB Slot Antenna Excited by Fork-Shaped Tuning Stub

Figure 3 shows the configuration of reference antenna 2. This antenna is a UWB slot antenna excited by a fork-shaped tuning stub. Compared with reference antenna 1, the circular radiator is removed. The feed line is described by parameter l_1 ($l_1 = 9.5$ mm) while other dimensions are kept as the same as reference antenna 1. A fork-shaped tuning stub is added to the feed line in order to achieve broad impedance matching. The dimensions of the fork-shaped tuning stub are set as follows: $t_1 = 7.5$ mm, $t_2 = 4$ mm, $t_3 = 0.4$ mm. A reflector is added to increase the directivity as well. Both reference antennas have the same size of the reflectors.

Figure 4 demonstrates the effect of various distances on the reflection coefficients versus frequency. It shows good performance of impedance matching at low frequency band though the impedance matching at high frequency band is poor. The bandwidth of the antenna becomes narrower when the distance d decreases.

It can be concluded that, both reference antennas have drawbacks. Reference antenna 1 has poor impedance matching at low frequency band while reference antenna 2 has poor impedance matching at high frequency band when the distance between the antenna and the reflector is very small. Our objective is to design a low profile antenna which can cover both low frequency band and high frequency band.

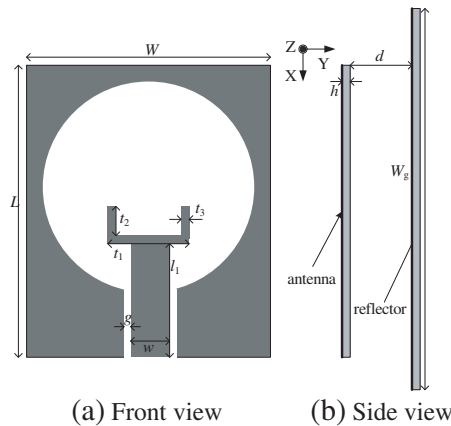


Figure 3. Configuration of reference directional UWB antenna with fork-shaped stub. (Reference Antenna 2).

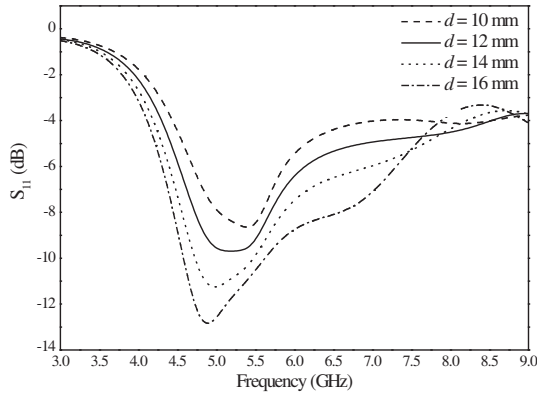


Figure 4. Simulated reflection coefficients in terms of d . (Reference Antenna 2).

3. CONFIGURATION AND DESIGN OF DIRECTIONAL UWB ANTENNA

3.1. Configuration of Proposed Directional UWB Antenna

Figure 5 shows the configuration of a novel directional UWB antenna. Compared with reference antenna 1, the slot ground and feed line are moved from top layer to bottom layer, and the feed line has been changed to fork-shaped tuning stub. The proposed antenna can also be viewed as a combination of reference antenna 2 on bottom layer and a circular patch on top layer, respectively. The dimension of the radiator is the same as reference antenna 1. For comparison, the dimensions of reflector are the same for three types of directional UWB antennas ($W_g = 50$ mm, $d = 12$ mm).

Figure 6 displays the reflection coefficients of proposed directional antenna compared with two reference antennas. It can be seen that, the proposed antenna has better impedance matching at low frequency band compared with reference antenna 1, due to the separation of the slot ground plane on the bottom layer from the circular patch on the top layer. Compared with reference antenna 2, the impedance matching of proposed antenna has been improved at high frequency band because of the added circular patch. The frequency band of proposed directional UWB antenna covers the frequency bands of both reference antenna 1 and reference antenna 2.

Figure 7 shows the comparison of antenna gain among three types of directional UWB antennas. It shows that, the antenna gain of the proposed antenna has the same variation trend with reference

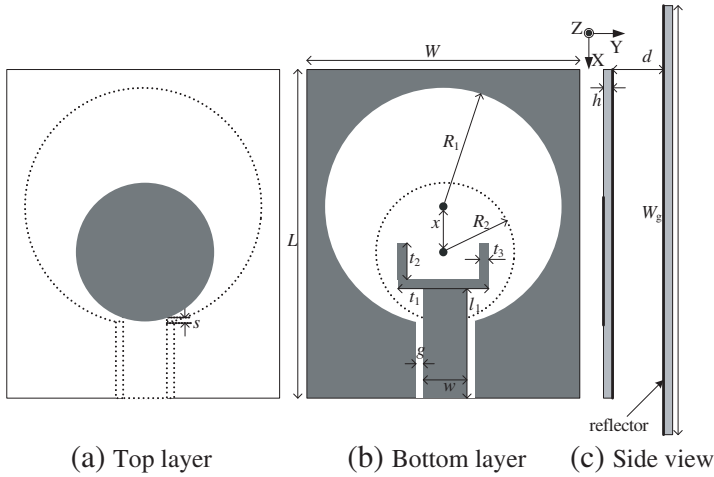


Figure 5. Configuration of proposed directional UWB antenna.

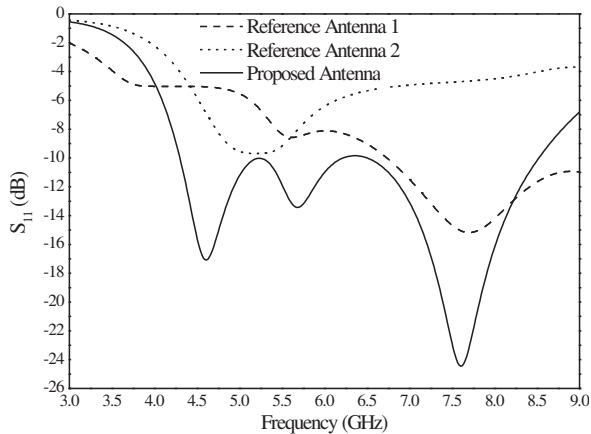


Figure 6. Simulated reflection coefficients among three types of antennas.

antenna 2 over the entire frequency band. The antenna gain of the proposed antenna is higher than reference antenna 2 over the entire frequency band due to the radiation of the circular patch. Compared with reference antenna 1, the antenna gain of the proposed antenna has been improved from 4 GHz to 6 GHz because of good impedance matching.

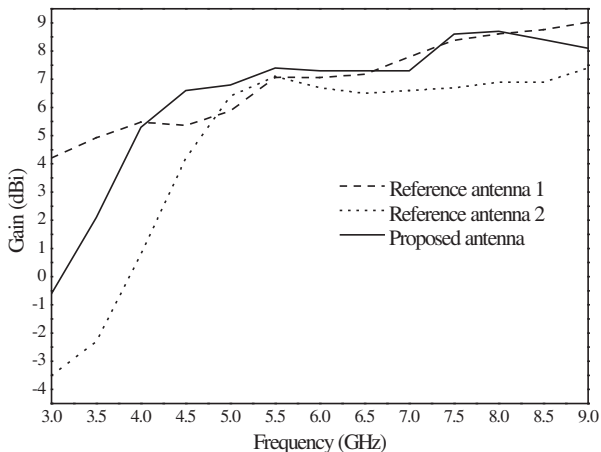


Figure 7. Simulated antenna gain among three types of directional UWB antennas.

3.2. Parametric Study of Proposed Directional UWB Antenna

Since this is a new design of directional UWB antenna, parametric study is performed to investigate the characteristics of the antenna. The commercial simulation tool Ansoft HFSS is employed to perform the design and optimization process.

Compared with reference antenna 2, the performance of the proposed antenna is improved due to the circular radiator. Hence, the radius of radiator R_2 is selected to perform the parametric study on the reflection coefficient.

Figure 8 shows the effect of circular radiator on the reflection coefficient. The circular slot is capable of supporting multiple resonant modes, and the overlapping of these multiple modes leads to the UWB characteristic [35]. When the radius of the radiator increases, the convergence of the first resonance and second resonance becomes poor. Small values of radius affect the convergence of the second resonance and the third resonance. The limiting case is that the proposed antenna changes to reference antenna 2 when the radius is zero and the impedance matching is found at low frequency band. The circular patch of the proposed antenna (shown in Fig. 5) plays a significant role as the gap between the circular radiator and the slot ground (shown in Fig. 1) and affects the combination of multi resonances.

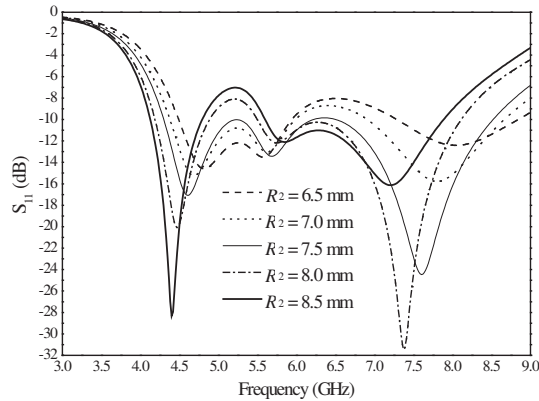


Figure 8. Simulated reflection coefficients in terms of R_2 .

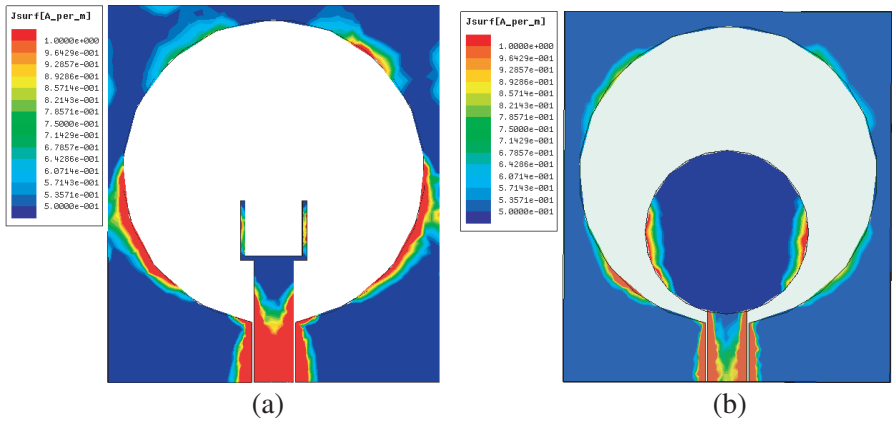


Figure 9. Simulated surface current distributions on the antenna at high frequency 8.5 GHz. (a) Reference Antenna 2. (b) Proposed Antenna.

3.3. Surface Current Distribution at High Frequency

Compared with reference antenna 2, the impedance matching of the proposed antenna is improved at high frequency band due to the added circular radiator. It can be explained via surface current distribution. Fig. 9 shows the simulated surface current distributions of reference antenna 2 and the proposed antenna at 8.5 GHz. It can be seen that, the surface current distribution concentrates near the feed line and half bottom of the ground plane when there is no circular patch. For the proposed antenna, the current is excited on the circular radiator

and it is accounting for the gain improvement compared with reference antenna 2. The added circular patch causes the spreading out of the surface current on the whole ground plane [36] and it will result in good performance of bandwidth broadening at higher frequencies.

4. SIMULATED AND MEASURED RESULTS

In order to verify the design of proposed directional UWB antenna, an antenna prototype (shown in Fig. 10) has been fabricated and tested in an anechoic chamber. The optimized dimensions of the proposed antenna are as follows: $W = 30$ mm, $L = 34$ mm, $R_1 = 13.7$ mm, $R_2 = 7.5$ mm, $x = 5.3$ mm, $w = 3.6$ mm, $g = 0.2$ mm, $l = 5.45$ mm, $s = 1.0$ mm, $W_g = 50$ mm, $d = 12$ mm. The antenna is fabricated on the Duroid5880 substrate with dielectric constant of 2.2 and thickness of 1.575 mm. The foam with dielectric constant of 1.0 and thickness of 12 mm is inserted in the space between antenna and reflector. Comparisons between simulated and measured reflection coefficients are shown in Fig. 11.

Both simulation and measurement demonstrate the good characteristic of impedance matching over a broad frequency band. Simulated and measured results confirm that the antenna features a reflection coefficient below -10 dB over the frequency range from 4.1 GHz to 8.9 GHz, which covers the designed frequency band.

The normalized radiation patterns in both the E -plane and H -plane have been examined at 4.2 GHz and 8.5 GHz as shown in Figs. 12(a)–(d). It shows reasonably good agreement between simulated and measured results. Directional patterns across the whole

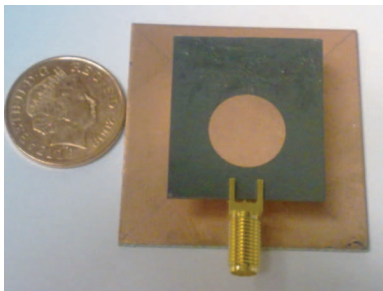


Figure 10. Photo of fabricated antenna prototype.

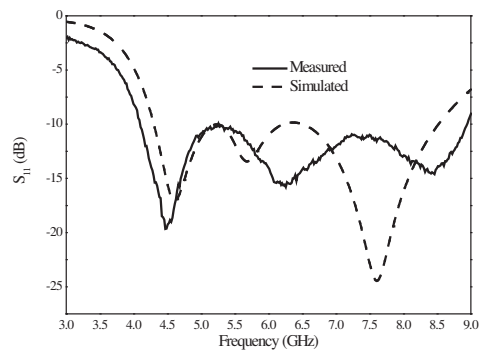


Figure 11. Measured and simulated reflection coefficients of the proposed directional UWB antenna.

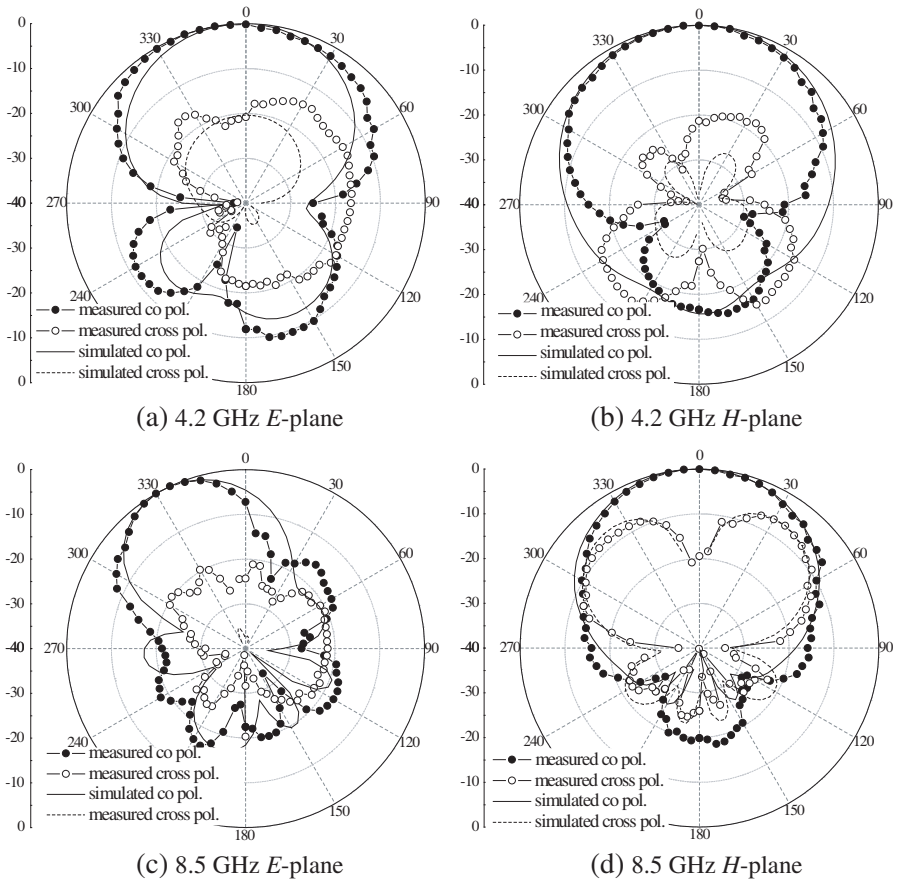


Figure 12. Measured and simulated radiation patterns at 4.2 and 8.5 GHz in the E -plane and H -plane.

operating band are achieved. The radiation patterns in the H -plane are stable and symmetrical over the whole frequency band. The radiation patterns in the E -plane are symmetrical at 4.2 GHz and the pattern at 8.5 GHz is shifted about 20° away from the broadside direction. This is due to the excitation of high order mode at 8.5 GHz which leads to the beam squinting. The front-to-back ratio over the UWB band is nearly 20 dB.

Figure 13 demonstrates the measured antenna gain at boresight versus frequency. The antenna gain at boresight is above 2.5 dBi over the entire frequency range. The antenna gain varies from 7.63 dBi to 2.54 dBi as the frequency increases from 5.5 GHz to 8.5 GHz. It is caused by the beam squinting problem.

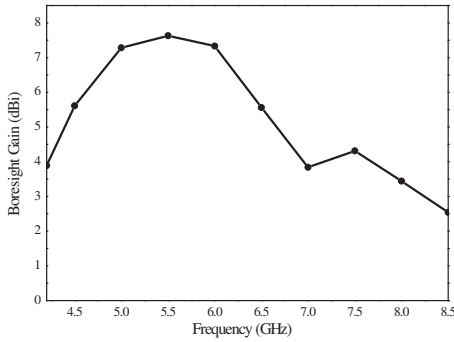


Figure 13. Measured antenna gain at boresight versus frequency.

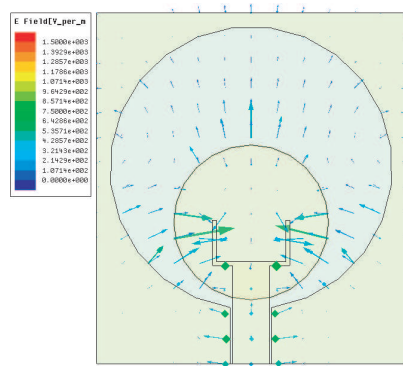


Figure 14. The electric field distribution of the resonant mode at 8.5 GHz.

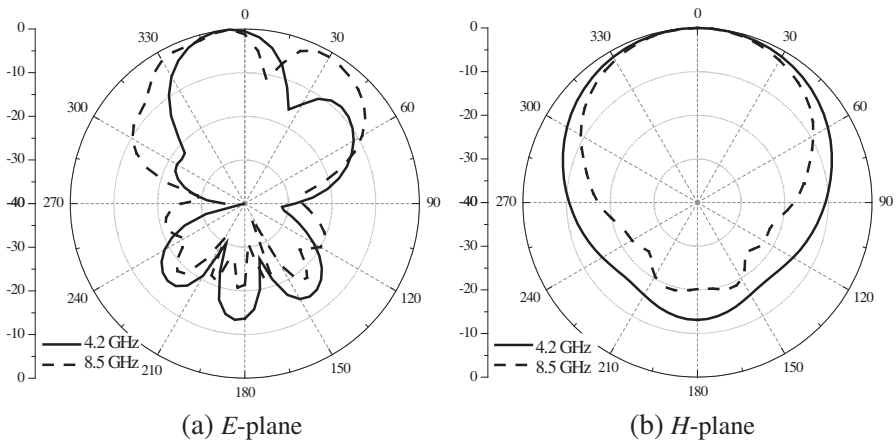


Figure 15. Simulated radiation patterns of two differential fed antenna elements placed in opposite directions.

The resonant mode plays an important role on the explanation of the radiation patterns at 8.5 GHz. Fig. 14 shows the electric field distribution corresponding to the resonant mode at 8.5 GHz, where the y -component fields are concentrated to the left and right sides of the circular patch. And the x -component fields are concentrated on the bottom of the circular slot. This field distribution contains higher order modes and makes the maximum direction of E -plane pattern shift from the boresight at 8.5 GHz, as shown in Fig. 12(c).

The beam squinting can be corrected by using an array of UWB

elements. For example, the radiation patterns of two UWB elements located in opposite directions can be combined to form the radiation at the boresight. The simulated radiation patterns of two elements placed in opposite directions are presented in Fig. 15. The phase offset is 180° between the two elements. It shows relative radiation patterns at different frequencies. The main beams keep stable at boresight at different frequencies.

It is worth noting that the simulations are implemented without RF feeding cables and lumped port is applied as excitation source in HFSS. In the measurements, an RF cable from the Vector Network Analyzer is connected to the SMA to excite the antenna. Agreement between simulations and measurements verifies that the RF feeding cable hardly affects the performance of the antenna.

Table 1 shows the performance of the directional UWB antenna including measured maximum gain, front-to-back ratio (FBR), co- to cross-polarization at the broadside and half power beam-width in the E -plane and H -plane. It shows that, the antenna has a maximum gain around 9 dBi and it has a high front-to-back ratio almost 20 dB. The cross-polarization increases at higher frequencies. In addition, the 3 dB beam-width in H -plane is wider than that in E -plane.

The last result concerns the ability of distortionless pulse transmission for the proposed directional UWB antenna. In this case, two identical proposed antennas are placed face to face by a separated distance of 20 cm. Two antennas are connected to the ports of Vector Network Analyzer (VNA). The differential Gaussian pulse is adopted [37]:

$$S(t) = \sin(2\pi f_0(t - t_0)) \exp(-(t - t_0)/\tau)^2 \quad (3)$$

where $f_0 = 6.3$ GHz, $\tau = 0.233$ ns, $t_0 = 4\tau$. The pulse covers the broad bandwidth extending from 4.2 GHz to 8.5 GHz. The S_{21}

Table 1. Performance of proposed directional UWB antenna.

f (GHz)	Gain (dBi)	FBR (dB)	Cross-pol. (dB)	HPBW ($^\circ$)	
				E	H
4.2	5.21	17.4	21.17	78	80
5	7.23	25.17	27.28	56	76
6	6.81	20.3	19.37	50	92
7	8.39	17.8	11.03	45	69
8	9.36	20.44	16.34	60	65
8.5	8.54	27.5	19.66	43	67

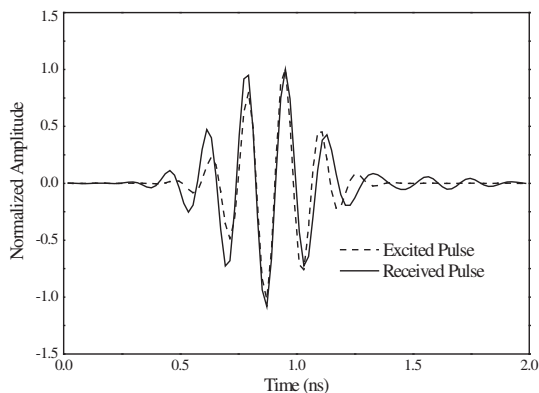


Figure 16. Measured impulse response of the antenna.

result measured by VNA represents the transfer function $H(f)$. The frequency response of the received pulse is $S(f)H(f)$. An inverse Fast Fourier Transform (IFFT) is used to convert the frequency response to the time domain. The measured result is shown in Fig. 16, where amplitudes of the transmitted and received pulses are normalized to have a peak value to 1. Both transmitted and received pulses are synchronized in the figure. The fidelity factor of the antenna is calculated using the same method presented in [38]. It is found to be larger than 90.5% which means that the proposed directional UWB antenna supports a nearly distortionless pulse transmission required for impulse radar system.

5. CONCLUSION

A novel directional UWB antenna has been introduced in this paper. The frequency band of the proposed antenna covers the band of OfCom from 4.2 to 8.5 GHz. Directional patterns, high front-to-back ratio (over 17 dB) and low cross-polarization have been realized. The principle of the antenna is explained. Three types of directional UWB antennas are analyzed and compared. Both frequency and time domain results are examined completely. The measured results confirm that it can feature a reflection coefficient below -10 dB from 4.1 GHz to 8.9 GHz, a maximum gain around 9.36 dBi, over 17 dB front-to-back ratio, and directional patterns. For the future work, the same method will be applied to design directional UWB antenna operating from 500 MHz to 3 GHz which is capable of penetrating through most common walls like thick concrete.

ACKNOWLEDGMENT

The project is supported by the funding from Surrey Space Centre, University of Surrey, UK, Department of Computing, University of Surrey, UK, and China Scholarship Council, P. R. China. Some measurements were carried out at the anechoic chamber of the Antenna Group at University of Bradford, UK. The authors would like to thank Prof. R. A. Abd-Alhameed for his help during the measurement.

REFERENCES

1. Withington, P., H. Fluhler, and S. Nag, "Enhancing homeland security with advanced UWB sensors," *IEEE Microw. Mag.*, 51–58, 2003.
2. Barnes, M. A., "Covert range gated wall penetrating motion sensor provides benefits for surveillance and forced entries," Time Domain Corporation, Huntsville, Alabama, 1999.
3. Nag, S., M. A. Barnes, T. Paymeng, and G. W. Holladay, "An ultra-wideband through-wall radar for detecting the motion of people in real time," *Proceedings of SPIE*, Vol. 4744, 2002.
4. http://www.cambridgeconsultants.com/prism_200.html.
5. <http://eurekaerospace.com/content/impulse-synthetic-aperture-radar-through-wall-and-underground-imaging>.
6. <http://www.camero-tech.com/product.php?ID=40>.
7. <http://www.novelda.no/>.
8. Yang, Y. and A. E. Fathy, "Development and implementation of a real-time see-through-wall radar system based on FPGA," *IEEE Trans. Geosci. Remote Sens.*, Vol. 47, No. 5, 1270–1280, 2009.
9. "New public safety applications and broadband internet access among uses envisioned by FCC authorization of UWB technology," Federal Communications Commission, February 14, 2002.
10. "Electronic communications — The wireless telegraphy (UWB equipment) Regulations 2007," *Statutory Instruments*, No. 2084, the Office of Communications, UK, July 20, 2007.
11. Chandra, R., A. N. Gaikwad, D. Singn, and M. J. Nigam, "An approach to remove the clutter and detect the target for ultra-wideband through-wall imaging," *J. Geophys. Eng.*, Vol. 5, 412–419, 2008.
12. Dehmollaian, M., M. Thiel, and K. Sarabandi, "Through-the-wall imaging using differential SAR," *IEEE Trans. Geosci. Remote Sens.*, Vol. 47, No. 5, 2009.

13. Yang, Y., C. Zhang, and A. E. Fathy, "Development and implementation of ultra-wideband see-through-wall imaging system based on sampling oscilloscope," *IEEE Antennas Wireless Propag. Lett.*, Vol. 7, 465–468, 2008.
14. Yang, Y., Y. Wang, and A. E. Fathy, "Design of compact Vivaldi antenna arrays for UWB see through wall applications," *Progress In Electromagnetics Research*, Vol. 82, 401–418, 2008.
15. Low, X. N., Z. N. Chen, and W. K. Toh, "Ultra-wideband suspended plate antenna with enhanced impedance and radiation performance," *IEEE Trans. Antennas Propag.*, Vol. 56, No. 8, 2490–2495, 2008.
16. Wong, H., K. M. Mak, and K. M. Luk, "Directional wideband shorted bowtie antenna," *Microw. Opt. Technol. Lett.*, Vol. 48, No. 8, 2006.
17. Wong, H., K. M. Mak, and K. M. Luk, "Wideband shorted bowtie patch antenna with electric dipole," *IEEE Trans. Antennas Propag.*, Vol. 56, No. 7, 2098–2111, 2008.
18. Chin, C. H. K., Q. Xue, and H. Wong "Broadband patch antenna with a folded plate pair as a differential feeding scheme," *IEEE Trans. Antennas Propag.*, Vol. 55, No. 9, 2461–2467, 2007.
19. Li, R., D. Thompson, M. M. Tentzeris, J. Laskar, and J. Papapolymerou, "Development of a wideband short backfire antenna excited by an unbalance-fed H -shaped slot," *IEEE Trans. Antennas Propag.*, Vol. 53, No. 2, 662–671, 2005.
20. Qu, S. W., J. L. Li, Q. Xue, and C. H. Chan, "Wideband cavity-backed bowtie antenna with pattern improvement," *IEEE Trans. Antennas Propag.*, Vol. 56, No. 12, 3850–3854, 2008.
21. Qu, S. W., C. H. Chan, and Q. Xue, "Ultra-wideband composite cavity-backed folded sectorial bowtie antenna with stable pattern and high gain," *IEEE Trans. Antennas Propag.*, Vol. 57, No. 8, 2478–2483, 2009.
22. Siu, L. and K. M. Luk, "Unidirectional antenna with loaded dielectric substrate," *IEEE Antennas Wireless Propag. Lett.*, Vol. 7, 50–53, 2008.
23. Elsherbini, A. and K. Sarabandi, "Directive coupled sectorial loops antenna for ultra-wideband applications," *IEEE Antennas Wireless Propag. Lett.*, Vol. 8, 576–579, 2009.
24. Kwag, Y. K., A. D. Hassanein, and D. J. Edwards, "A high-directive bowtie radar antenna with a pyramidal reflector for ultra-wideband radar imaging applications," *Microw. Opt. Technol. Lett.*, Vol. 51, No. 2, 387–390, 2009.

25. Midrio, M., S. Boscolo, F. Sacchetto, F. M. Pigozzo, and A. D. Capobianco, "Novel ultra-wideband bow tie antenna with high front-to-back ratio and directivity," *Microw. Opt. Technol. Lett.*, Vol. 52, No. 5, 1016–1020, 2010.
26. Ito, Y., M. Ameya, M. Yamamoto, and T. Nojima, "Unidirectional UWB array antenna using leaf-shaped bowtie elements and flat reflector," *Electron. Lett.*, Vol. 44, No. 1, 2008.
27. Habib, M. A., A. Bostani, A. Djaiz, M. Nedil, M. C. E. Yagoubm, and T. A. Denidni, "Ultra wideband cpw-fed aperture antenna with WLAN band rejection," *Progress In Electromagnetics Research*, Vol. 106, 17–31, 2010.
28. Barbarino, S. and F. Consoli, "UWB circular slot antenna provided with an inverted-L notch filter for the 5 GHz WLAN band," *Progress In Electromagnetics Research*, Vol. 104, 1–13, 2010.
29. Chen, D. and C.-H. Cheng, "A novel compact ultra-wideband (UWB) wide slot antenna with via holes," *Progress In Electromagnetics Research*, Vol. 94, 343–349, 2009.
30. Hu, Y.-S., M. Li, G.-P. Gao, J.-S. Zhang, and M.-K. Yang, "A double-printed trapezoidal patch dipole antenna for UWB applications with band-notched characteristic," *Progress In Electromagnetics Research*, Vol. 103, 259–269, 2010.
31. Abbosh, A. M., M. E. Bialkowski, J. Mazierska, and M. V. Jacob, "A planar UWB antenna with signal rejection capability in the 4–6 GHz band," *IEEE Microw. Wireless Compon. Lett.*, Vol. 16, No. 5, 2006.
32. Ren, Y. J., C. P. Lai, P. H. Chen, and R. M. Narayanan, "Compact ultra-wideband UHF array antenna for through-wall radar applications," *IEEE Antennas Wireless Propag. Lett.*, Vol. 8, 1302–1305, 2009.
33. Klemm, M., I. Z. Kovcs, G. F. Pedersen, and G. Troster, "Novel small-size directional antenna for UWB WBAN/WPAN applications," *IEEE Trans. Antennas Propag.*, Vol. 53, No. 12, 3884–3896, 2005.
34. Lin, Y. C. and K. J. Hung, "Compact ultra-wideband rectangular aperture antenna and band-notched designs," *IEEE Trans. Antennas Propag.*, Vol. 54, No. 11, 3075–3081, 2006.
35. Allen, B., M. Dohler, E. E. Okon, W. Q. Malik, A. K. Brown, and D. J. Edwards, *Ultra-wideband Antennas and Propagation for Communications, Radar and Imaging*, 134–135, Wiley, 2007.

36. Chen, C. C. and J. L. Volakis, "Bandwidth broadening of patch antennas using non-uniform substrates," *Microw. Opt. Tech. Lett.*, Vol. 47, No. 5, 421–423, 2005.
37. Chung, S. W. J., R. A. Abd-Alhameed, C. H. See, and P. S. Excell, "Wideband loaded wire bow-tie antenna for near field imaging using genetic algorithms," *PIERS Online*, Vol. 4, No. 5, 591–595, 2008.
38. Yang, Y. Y., Q. X. Chu, and Z. A. Zheng, "Time domain characteristics of band-notched ultra-wideband antenna," *IEEE Trans. Antennas Propag.*, Vol. 57, No. 10, 3426–3430, 2009.